

Self-diffusive dynamics of active Brownian particles at moderate densities

Rodrigo Soto^{a)}

Departamento de Física, Facultad de Ciencias Físicas y Matemáticas, Universidad de Chile, Santiago, Chile

(Dated: 11 March 2025)

The Active Brownian Particle (ABP) model has become a prototype of self-propelled particles. ABPs move persistently at a constant speed V along a direction that changes slowly by rotational diffusion, characterized by a coefficient D_r . Persistent motion plus random reorientations generate a random walk at long times with a diffusion coefficient that, for isolated ABPs in two dimensions, is given by $D_0 = V^2/(2D_r)$. Here we study the density effects on the self-diffusive dynamics using a recently proposed kinetic theory for ABPs, in which persistent collisions are described as producing a net displacement on the particles. On intermediate timescales, where many collisions have taken place but the director of the tracer particle has not yet changed, it is possible to solve the Lorentz kinetic equation for a tracer particle. It turns out that, as a result of collisions, the tracer follows an effective stochastic dynamics, characterized by an effective reduced streaming velocity V_{eff} and anisotropic diffusion, with coefficients explicitly depending on the density. Based on this result, an effective theoretical and numerical approach is proposed in which the particles in a bath follow stochastic dynamics with mean-field interactions based on the local density. Finally, on time scales larger than D_r^{-1} , studying the van Hove function at small wavevectors, it is shown that the tracer particle presents an effective diffusive motion with a coefficient $D = V_{\text{eff}}^2/(2D_r)$. The dependence of V_{eff} on the density indicates that the kinetic theory is limited to area fractions smaller than 0.42, and beyond this limit unphysical results appear.

I. INTRODUCTION

Self-propelled particles such as swimming bacteria, mesenchymal cells, active colloids, or microrobots move persistently along directions that change randomly on long time scales¹. Bacteria and other flagellated microorganisms change their director in tumbling events, where a new director is randomly chosen to start a new run phase^{2,3}. In mesenchymal cells, active direction reversal occurs when the cell comes into contact with another cell in a process called contact inhibition of locomotion⁴. Active colloids and microrobots normally change their direction continuously only by rotational diffusion^{5,6}. In fact, rotational diffusion is also present in swimming bacteria and mesenchymal cells, which is superimposed on the other active reorientation processes. In general, the intensity of rotational diffusion need not be thermal, as other processes may be in action. In any case, the combination of persistent motion and random reorientations generates an effective random walk for isolated swimmers. Dimensional analysis shows that the diffusion coefficient should scale as $D_0 \sim V^2/\tau$, where V is the self-propulsion speed and τ is the average persistence time. The quantitative calculation of the prefactor has been accurately obtained for run-and-tumble bacteria^{2,3}, bacteria with long internal chemotactic memory⁷, active colloids⁸, and several extensions of these models^{9–12}.

Since rotational diffusion is a general mechanism present in self-propelled particles, it becomes relevant to isolate this mechanism to study its effects. The Active

Brownian Particle (ABP) model has emerged as a prototype of self-propelled particles where the director changes only by rotational diffusion and the particles interact only through excluded volume^{10,13,14}. In its simplest form, the position \mathbf{r}_i and the director $\hat{\mathbf{n}}_i$ of the i -th particle evolve as

$$\dot{\mathbf{r}}_i = V\hat{\mathbf{n}}_i + \mathbf{F}_i/\gamma, \quad (1)$$

$$\dot{\hat{\mathbf{n}}}_i = \sqrt{2D_r}\boldsymbol{\xi}_i(t) \times \hat{\mathbf{n}}_i, \quad (2)$$

where $\boldsymbol{\xi}_i$ are vectorial white noises of correlation $\langle \xi_{\mu,i}(t)\xi_{\nu,j}(t') \rangle = \delta_{\mu,\nu}\delta_{i,j}\delta(t-t')$, with $\mu, \nu = x, y, z$, the Cartesian coordinates. Here, $\mathbf{F}_i = -\frac{\partial U}{\partial \mathbf{r}_i}$ is the hard-core interparticle force acting on i , where U is the potential energy, γ is the mobility coefficient, which is assumed to be constant, and D_r is the rotational diffusion coefficient. The dynamics of ABPs is non-inertial, reflecting the motion of microscopic particles moving at low Reynolds number.

In the following, although much of the discussion applies to arbitrary spatial dimensions, we will concentrate on the two-dimensional case, which is experimentally relevant since active colloids are usually non-buoyant and sediment to the bottom of the observation box. In this case, the director is simply characterized by an angle for each particle $\hat{\mathbf{n}}_i = (\cos \phi_i, \sin \phi_i)$, which evolves as

$$\dot{\phi}_i = \sqrt{2D_r}\xi_i(t), \quad (3)$$

with ξ_i white noises of correlation $\langle \xi_i(t)\xi_j(t') \rangle = \delta_{i,j}\delta(t-t')$. In the limit of hard-core interactions, with diameter σ , a collection of N ABPs moving in a two-dimensional box of area A is characterized by two dimensionless parameters: the area fraction $\eta = \pi\sigma^2\rho_0/4$, where $\rho_0 = N/A$ is the number density, and the Péclet

^{a)}Electronic mail: rsoto@uchile.cl

number $Pe = V/(\sigma D_r)$, which quantifies the persistence of the particles. More specifically, Pe compares the time it takes for the particle to change direction, D_r^{-1} , with the time it takes for a particle to travel its size, σ/V .

A quite striking feature of ABPs is that, for sufficiently large densities and persistence, they exhibit a phase separation forming large clusters, even though their interaction is purely repulsive^{15–19}. The origin of this motility induced phase separation (MIPS) is that in a dense medium, particles tend to move at a reduced velocity due to collisions. The velocity reduction depends on density and can trigger a density instability^{20,21}. Recently, a kinetic equation has been proposed to describe the dynamics of a collection of ABPs at high Péclet number, correctly predicting the area fraction to generate MIPS based on purely microscopic arguments²². The idea behind this kinetic theory is that collisions take a finite time due to persistence. If $Pe \gg 1$, the directors do not change during the encounter, but the collision has a net effect of displacing the particles (see Fig. 1a). These displacements are obtained as the difference between the actual positions at the end of the collision and the positions they would have had in the absence of the event.

Despite the importance of the model, the diffusion process for dense ABP systems has received little attention. Ref. 23 presents numerical results on the density dependence of the self-diffusion coefficient. As an effect of crowding, it shows a decreasing tendency with increasing density. Using a mode-coupling theory, the self-diffusion coefficient is computed theoretically and it also shows that it decreases with density²⁴. In both cases, however, no expression for the density dependence is given.

In this article, we use the kinetic theory discussed above to compute the diffusive dynamics in moderately dense systems. Special attention is given to finding explicit expressions for the density dependence of the various transport coefficients. The article is organized as follows. Section II revisits the kinetic equation derived in Ref. 22 and discusses the possible approximations for the pair correlation function at contact. The kinetic equation for a tagged particle moving in a system of ABPs is derived in Sect. III and the different time regimes are introduced. The analysis of the self-diffusion process of the tagged particle is performed in Sects. IV and V for the intermediate and long time regimes, respectively. In both cases, the effective diffusion coefficients and the effective streaming velocity are obtained. Finally, the conclusions are presented in Sect. VI.

II. KINETIC DESCRIPTION FOR A GAS OF ABPS

In the kinetic language, a collection of ABPs is described by the distribution function $f(\mathbf{r}_1, \hat{\mathbf{n}}_1, t)$, which gives the number of particles in the vicinity of \mathbf{r}_1 and director $\hat{\mathbf{n}}_1$, at time t . The distribution function is nor-

malized so that

$$\rho(\mathbf{r}_1, t) = \int f(\mathbf{r}_1, \hat{\mathbf{n}}_1, t) d\hat{\mathbf{n}}_1 \quad (4)$$

is the number density. In Ref. 22, it is shown that the evolution of f is given by a Boltzmann-like equation

$$\frac{\partial f}{\partial t} + V \hat{\mathbf{n}}_1 \cdot \frac{\partial}{\partial \mathbf{r}_1} f = D_r \nabla_{\hat{\mathbf{n}}_1}^2 f + J[f], \quad (5)$$

where the left-hand side (l.h.s.) describes the free motion of the particles with velocity $V \hat{\mathbf{n}}_1$ and the first term of the right-hand side (r.h.s.) accounts for the rotational diffusion of the director. J is a term that accounts for the change in the distribution function due to collisions. To build J an approach similar to the Boltzmann equation is used^{25,26}. That is, the average collision rate is computed from the distribution function, and for each collision, the change in f is obtained independently. Finally, J is obtained by integrating over all possible collision parameters.

A collision here is the encounter of two ABPs with directors $\hat{\mathbf{n}}_1$ and $\hat{\mathbf{n}}_2$, which are separated at the beginning of the collision by the vector $\sigma \hat{\boldsymbol{\sigma}}$ that goes from particle 1 to 2 (see Fig. 2 in the Appendix). With this parametrization, the number of collisions per unit time is $f^{(2)}(\mathbf{r}_1, \hat{\mathbf{n}}_1, \mathbf{r}_2, \hat{\mathbf{n}}_2)|_{|\mathbf{r}_1 - \mathbf{r}_2| = \sigma} |\sigma V(\hat{\mathbf{n}}_2 - \hat{\mathbf{n}}_1) \cdot \hat{\boldsymbol{\sigma}}| \Theta[-(\hat{\mathbf{n}}_2 - \hat{\mathbf{n}}_1) \cdot \hat{\boldsymbol{\sigma}}]$, where $f^{(2)}$ is the two-particle distribution function that gives the number of pairs of particles having simultaneously positions and directors in the vicinity of $\mathbf{r}_1, \hat{\mathbf{n}}_1, \mathbf{r}_2$, and $\hat{\mathbf{n}}_2$. The factor $|\sigma V(\hat{\mathbf{n}}_2 - \hat{\mathbf{n}}_1) \cdot \hat{\boldsymbol{\sigma}}|$ takes into account that the collision rate is proportional to the particle size and the relative velocity normal to the relative vector. Finally, the Heaviside step function Θ selects particles that are approaching. Using this collision rate would lead to a non-closed equation with the r.h.s. depending on $f^{(2)}$. To close the equation, we first write

$$f^{(2)}(\mathbf{r}_1, \hat{\mathbf{n}}_1, \mathbf{r}_2, \hat{\mathbf{n}}_2) = g^{(2)}(\mathbf{r}_1, \hat{\mathbf{n}}_1, \mathbf{r}_2, \hat{\mathbf{n}}_2) f(\mathbf{r}_1, \hat{\mathbf{n}}_1) f(\mathbf{r}_2, \hat{\mathbf{n}}_2), \quad (6)$$

which defines the pair correlation function $g^{(2)}$. We recall that it must be evaluated only with the two particles in contact and approaching, that is, in a precollisional state, defining the pair correlation function at contact $\chi \equiv \lim_{r_{12} \rightarrow \sigma} g^{(2)}(\mathbf{r}_1, \hat{\mathbf{n}}_1, \mathbf{r}_2, \hat{\mathbf{n}}_2)|_{(\hat{\mathbf{n}}_2 - \hat{\mathbf{n}}_1) \cdot (\mathbf{r}_2 - \mathbf{r}_1) < 0}$. The classical molecular chaos hypothesis consists on assuming $\chi = 1$. In dense gases of hard spheres particles it is common to go beyond this crude approximation and use the Enskog approach, which consists in assuming that $g^{(2)}$ at contact is given by the distribution at equilibrium, implying that χ depends only on the density profile^{25–27}. In granular gases, as a consequence of the longer times particles remain in contact as an effect of inelasticity, $g^{(2)}$ shows a large angular dependence for the postcollisional states, but for the precollisional states χ is very well approximated by the equilibrium expression for hard elastic spheres^{28,29}. Also, there is a strong discontinuity at the

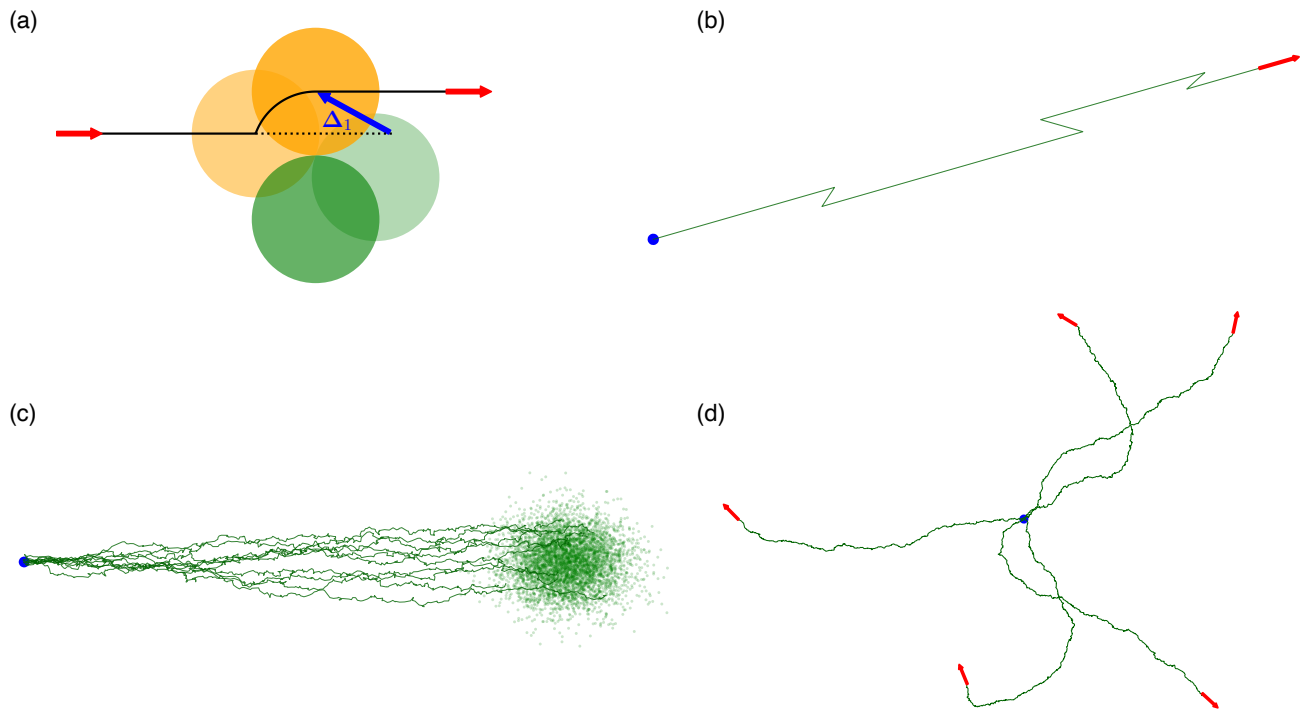


FIG. 1. Schematic representation of the particle dynamics at different timescales. The red arrow represents the director and the blue circle the initial position. (a) Elementary collision process in which a particle moving to the right (orange) collides with another particle (green). The solid black line shows the actual trajectory and the dotted black line shows the trajectory in absence of the collision. The blue arrow shows the effective displacement Δ_1 produced by the collision. (b) Effective trajectory after a few collisions for $t_{\text{col}}, t_{\text{free}} \lesssim t \ll t_{\text{rot}}$. (c) Effective Brownian dynamics for $t_{\text{col}}, t_{\text{free}} \ll t \ll t_{\text{rot}}$, implying that the director is fixed pointing to the right. Example trajectories, obtained by numerically solving Eq. (23) with $D_r = 0$, are shown in dark green, and the light green dots indicate the final positions, where it can be seen that $D_{\parallel} > D_{\perp}$. (d) Effective Brownian dynamics valid for $t_{\text{rot}} \lesssim t$, allowing the director to change. The sample trajectories are obtained by numerically solving Eq. (23) with a finite value for D_r .

transition between the pre- and post-collisional states, i.e. for grazing encounters³⁰. Even for a simple homogeneous and isotropic state, the pair distribution function $g^{(2)}$ for ABPs depends in principle on the relative distance $r = |\mathbf{r}_1 - \mathbf{r}_2|$ and two angles. The measurements in Refs. 31 and 32 show important angular dependencies, but the authors did not separate pre- and postcollisional states, and therefore the measured values of $g^{(2)}$ cannot be used for a collision theory of ABPs. Therefore, in the absence of a validated expression, we will present the results in terms of a general χ , but assuming that it depends only on the local density and not on the angles. For explicit calculations, the elastic hard disk expression $\chi_{\text{hd}} = (1 - 7\eta/16)/(1 - \eta)^2$ is used, where $\eta = \pi\sigma^2\rho_0/4$ is the area fraction^{22,33}.

When two particles meet, they slide until they reach a grazing configuration $(\hat{\mathbf{n}}_2 - \hat{\mathbf{n}}_1) \cdot \hat{\boldsymbol{\sigma}} = 0$, at which point they begin to move apart. In the limit Pe going to infinity, the two particles kept their directors unchanged and it is direct to integrate the equations of motion of the two particles and obtain their final positions $\mathbf{r}_{1,2}^{\text{end}}$ and the duration of the collision Δt^{col} . In absence of the collision, the final positions would have been the result of free mo-

tion, $\mathbf{r}_{1,2}^{\text{ini}} + V\hat{\mathbf{n}}_{1,2}\Delta t^{\text{col}}$. Then the whole collision process can be interpreted as the particles being instantaneously displaced a distance $\Delta_{1,2} \equiv \mathbf{r}_{1,2}^{\text{end}} - (\mathbf{r}_{1,2}^{\text{ini}} + V\hat{\mathbf{n}}_{1,2}\Delta t^{\text{col}})$, while keeping the directors unchanged. Explicit expressions for the effective displacements $\Delta_{1,2}$ in terms of $\hat{\mathbf{n}}_{1,2}$ and $\hat{\boldsymbol{\sigma}}$, obtained in Ref. 22, are also given in the Appendix.

Considering all these elements, J is written as a Boltzmann–Enskog-like collision term

$$J[f] = \int \chi \left(\rho \left(\frac{\mathbf{r}'_1 + \mathbf{r}'_2}{2} \right) \right) f(\mathbf{r}'_1, \hat{\mathbf{n}}_1) f(\mathbf{r}'_2, \hat{\mathbf{n}}_2) \times |V\sigma^{d-1}(\hat{\mathbf{n}}_2 - \hat{\mathbf{n}}_1) \cdot \hat{\boldsymbol{\sigma}}| \Theta[-(\hat{\mathbf{n}}_2 - \hat{\mathbf{n}}_1) \cdot \hat{\boldsymbol{\sigma}}] \delta(\mathbf{r}'_2 - \mathbf{r}'_1 - \sigma\hat{\boldsymbol{\sigma}}) \times [\delta(\mathbf{r}_1 - \mathbf{r}'_1 - \Delta_1) - \delta(\mathbf{r}_1 - \mathbf{r}'_1)] d\mathbf{r}'_1 d\mathbf{r}'_2 d\hat{\mathbf{n}}_2 d\hat{\boldsymbol{\sigma}}. \quad (7)$$

It accounts for the effective displacement Δ_1 of the tagged particle due to collisions with another particle of director $\hat{\mathbf{n}}_2$. The loss term [associated with the Dirac delta $\delta(\mathbf{r}_1 - \mathbf{r}'_1)$] describes a particle at position \mathbf{r}_1 that collides with a partner, while the gain term, associated to the Dirac delta $\delta(\mathbf{r}_1 - \mathbf{r}'_1 - \Delta_1)$, describes a particle that was at $\mathbf{r}_1 - \Delta_1$ and ends at \mathbf{r}_1 after the collision. In both cases, the partner is at a distance $\sigma\hat{\boldsymbol{\sigma}}$ from the

tagged particle. Finally, we recall that the collision term (7) describes the dynamics in the limit of very large Pe, implying that the director $\hat{\mathbf{n}}_1$ of the tagged particle does not change during a collision.

III. KINETIC EQUATION FOR A TRACER PARTICLE

To study the self-diffusion process, we consider a system of ABPs with number density ρ_0 , in two spatial dimensions. The system is at equilibrium, described by an isotropic and homogeneous distribution function $f_0 = \rho_0/(2\pi)$. In the system, there is a tracer, a tagged particle, mechanically equal to the others. The motion of the tracer is described by the kinetic equation (5), where in the collision term the tagged particle is described by an inhomogeneous and time-dependent distribution f , while the partners are described by the bath distribution f_0 . Under these conditions, since f_0 does not depend on the position or the director, the collision term simplifies enormously and becomes a linear operator on f , called the Lorentz collision operator

$$J_L[f] = \frac{\rho_0\chi_0\sigma}{2\pi} \int [f(\mathbf{r}_1 - \mathbf{\Delta}_1, \hat{\mathbf{n}}_1) - f(\mathbf{r}_1, \hat{\mathbf{n}}_1)] \times |V(\hat{\mathbf{n}}_2 - \hat{\mathbf{n}}_1) \cdot \hat{\boldsymbol{\sigma}}| \Theta[-(\hat{\mathbf{n}}_2 - \hat{\mathbf{n}}_1) \cdot \hat{\boldsymbol{\sigma}}] d\hat{\mathbf{n}}_2 d\hat{\boldsymbol{\sigma}}. \quad (8)$$

With this, the evolution of f for the tracer is given by the Boltzmann–Lorentz equation

$$\frac{\partial f}{\partial t} + V\hat{\mathbf{n}}_1 \cdot \frac{\partial}{\partial \mathbf{r}_1} f = D_r \nabla_{\hat{\mathbf{n}}_1}^2 f + J_L[f]. \quad (9)$$

The collision term can be easily interpreted as a loss and a gain term. For the loss term, the tagged particle is collided by others causing it to be removed from its original position \mathbf{r}_1 . The gain term, on the other hand, describes a tagged particle that was located at $\mathbf{r}_1 - \mathbf{\Delta}_1$, where the collision produces a net displacement $\mathbf{\Delta}_1$, resulting in it ending up at \mathbf{r}_1 after the collision. As in the full equation (7), the factor $|V(\hat{\mathbf{n}}_2 - \hat{\mathbf{n}}_1) \cdot \hat{\boldsymbol{\sigma}}|$ indicates that the collision rate is proportional to the relative velocity and $\Theta[-(\hat{\mathbf{n}}_2 - \hat{\mathbf{n}}_1) \cdot \hat{\boldsymbol{\sigma}}]$ selects only particles that are approaching. Finally, for both processes the collision frequency is proportional to $\rho_0\chi_0\sigma$, where χ_0 is the pair correlation function at contact evaluated at the global density. In two spatial dimensions, directors are characterized by a single angle $\hat{\mathbf{n}} = (\cos\phi, \sin\phi)$ and the unit vector $\hat{\boldsymbol{\sigma}}$ is parametrized by the angle θ it makes with $\hat{\mathbf{n}}_2 - \hat{\mathbf{n}}_1$, such that $\cos\theta < 0$. More details on the parametrization of the integrals is given in the Appendix.

The resulting kinetic equation for the tracer (8) and (9), although linear, is complex to analyze under general conditions due to its intrinsic non-locality in space and the involved integrals in the angles. We will study the dynamics at times longer than the characteristic scale of collisions $t_{\text{col}} = \sigma/V$ and the mean free time $t_{\text{free}} = 1/(\rho_0\chi_0V\sigma)$, where many individual collision events have taken place. Another relevant time scale is the rotational

diffusion time $t_{\text{rot}} = 1/D_r$, which characterizes the time for an ABP to forget its direction. Two cases will be studied, first the intermediate time scale $t_{\text{col}}, t_{\text{free}} \ll t \ll t_{\text{rot}}$, where the tracer preserves its director but nevertheless it has experienced several collisions. Second, the long time regime, $t_{\text{rot}} \ll t$, is analyzed, in which case the tracer has completely forgotten its original direction and the motion is purely diffusive. See Fig. 1 for a schematic representation of the different timescales.

To study the spatio-temporal evolution of f , we work with the Fourier–Laplace transform, which is defined for any function $A(\mathbf{r}, t)$ as

$$\tilde{A}(\mathbf{k}, s) = \int_0^\infty dt e^{-st} \int d^2r e^{-i\mathbf{k}\cdot\mathbf{r}} A(\mathbf{r}, t). \quad (10)$$

Especially relevant is the Fourier–Laplace transform of the density

$$\tilde{\rho}(\mathbf{k}, s) = \int \tilde{f}(\mathbf{k}, \hat{\mathbf{n}}, s) d\hat{\mathbf{n}}, \quad (11)$$

also known as the van Hove function. For example, if the density is described by a simple diffusion equation in the small wavevector regime, then the van Hove function is given by $\tilde{\rho}(\mathbf{k}, s) = 1/(s + Dk^2)$, which is a direct way to obtain the diffusion coefficient by simple inspection³⁴. Note that the van Hove function is normalized to one, since there is a single tagged particle.

IV. EFFECTIVE DYNAMICS AT INTERMEDIATE TIME SCALES

To analyze the dynamics at the intermediate time scale, where rotational diffusion has not been effective in changing the tracer director, we take $D_r = 0$ in the kinetic equation and set as initial condition that the tracer is placed at the origin and has a well-defined direction, which is chosen to be $\phi = 0$, meaning that $\hat{\mathbf{n}} = \hat{\mathbf{x}}$. That is,

$$f(\mathbf{r}, \hat{\mathbf{n}}, t = 0) = \delta(\mathbf{r})\delta(\phi). \quad (12)$$

Suppressing rotational diffusion eliminates the only mechanism for changing direction and therefore $\phi = 0$ for all times, implying that the tracer distribution function can be written as

$$f(\mathbf{r}, \hat{\mathbf{n}}, t) = \rho(\mathbf{r}, t)\delta(\phi). \quad (13)$$

Here $\rho(\mathbf{r}, t)$ is the density, with the initial condition $\rho(\mathbf{r}, t = 0) = \delta(\mathbf{r})$, which corresponds to the so-called van Hove process. Substituting Eq. (13) for f in Eq. (9) and making a Laplace–Fourier transform of the equation gives

$$s\tilde{\rho} - 1 + iV\mathbf{k} \cdot \hat{\mathbf{x}}\tilde{\rho} = \Phi\tilde{\rho} \int [e^{-i\mathbf{k}\cdot\mathbf{\Delta}_1} - 1] dX, \quad (14)$$

where $\Phi = \rho_0 \chi V \sigma / (2\pi)$, $dX = |(\hat{\mathbf{n}}_2 - \hat{\mathbf{n}}_1) \cdot \hat{\boldsymbol{\sigma}}| \Theta[-(\hat{\mathbf{n}}_2 - \hat{\mathbf{n}}_1) \cdot \hat{\boldsymbol{\sigma}}] |_{\phi_1=0} d\phi_2 d\theta$, and the factor $\delta(\phi_1)$ was simplified in all terms. Note that in the third term in the l.h.s. we use that $\hat{\mathbf{n}} = \hat{\mathbf{x}}$ and therefore the streaming part depends only on k_x .

The van Hove function is therefore given by $\tilde{\rho}(\mathbf{k}, s) = [s + iV k_x + \Phi I]^{-1}$, where

$$I = \int [1 - e^{-i\mathbf{k} \cdot \boldsymbol{\Delta}_1}]_{\phi_1=0} dX \\ = \int \left[i\mathbf{k} \cdot \boldsymbol{\Delta}_1 + \frac{\mathbf{k}\mathbf{k}}{2} : \boldsymbol{\Delta}_1 \boldsymbol{\Delta}_1 + \dots \right]_{\phi_1=0} dX. \quad (15)$$

The collisional integral I has been expanded in k to analyze the long wavelength dynamics, stopping at order k^2 , meaning that we analyze the streaming and diffusive behavior. Since $\phi_1 = 0$ fixes a preferred direction, by symmetry arguments we have

$$\int \boldsymbol{\Delta}_1 |_{\phi_1=0} dX = A \hat{\mathbf{x}}, \quad (16a)$$

$$\frac{1}{2} \int \boldsymbol{\Delta}_1 \boldsymbol{\Delta}_1 |_{\phi_1=0} dX = B \hat{\mathbf{x}} \hat{\mathbf{x}} + C \hat{\mathbf{y}} \hat{\mathbf{y}}. \quad (16b)$$

From these expressions we get

$$A = \int (\boldsymbol{\Delta}_1 \cdot \hat{\mathbf{x}}) |_{\phi_1=0} dX = -\frac{\pi^2 \sigma}{2} \approx -4.93\sigma, \quad (17a)$$

$$B = \frac{1}{2} \int (\boldsymbol{\Delta}_1 \cdot \hat{\mathbf{x}})^2 |_{\phi_1=0} dX = \frac{2(12G - 1)\sigma^2}{9} \approx 2.22\sigma^2, \quad (17b)$$

$$C = \frac{1}{2} \int (\boldsymbol{\Delta}_1 \cdot \hat{\mathbf{y}})^2 |_{\phi_1=0} dX = \frac{2(6G + 1)\sigma^2}{9} \approx 1.44\sigma^2, \quad (17c)$$

where $G \approx 0.92$ is the Catalan's constant, and the integrals were computed using the methods described in the Appendix.

Collecting all terms and going back to a general fixed director $\hat{\mathbf{n}}$, the van Hove function is finally

$$\tilde{\rho}(\mathbf{k}, s) = [s + i\mathbf{k} \cdot V_{\text{eff}} \hat{\mathbf{n}} + \Phi B (\mathbf{k} \cdot \hat{\mathbf{n}})^2 + \Phi C (\mathbf{k} \cdot \hat{\mathbf{t}})^2]^{-1}, \quad (18)$$

where $\hat{\mathbf{t}}$ is the unit vector transversal to $\hat{\mathbf{n}}$ and

$$V_{\text{eff}} = V + \Phi A = (1 - \eta \chi_0) V \quad (19)$$

is the effective speed, which was previously found using an heuristic analysis of the kinetic equation²². The decrease of the effective velocity with density is at the basis of the MIPS theory, where expressions similar to Eq. (19) have been proposed based on semiempirical methods^{14,35} or derived in the limiting case of infinite spatial dimensions³⁶. Here it emerged as an effect of the collisions without the need to impose it. By inspection, it is possible to identify the van Hove function (18) as the solution of the anisotropic advection-diffusion equation for

the density

$$\frac{\partial \rho}{\partial t} + V_{\text{eff}} \hat{\mathbf{n}} \cdot \nabla \rho = D_{\parallel} (\hat{\mathbf{n}} \cdot \nabla)^2 \rho + D_{\perp} (\hat{\mathbf{t}} \cdot \nabla)^2 \rho, \quad (20)$$

where $D_{\parallel} = \Phi B$ and $D_{\perp} = \Phi C$ are the longitudinal and transversal diffusion coefficients, respectively, which we note are different, being the longitudinal one larger. With their density dependence through Φ ,

$$D_{\parallel} = \frac{4(12G - 1)\sigma^2}{9\pi^2} \eta \chi_0 V \sigma \approx 0.45 \eta \chi_0 V \sigma, \quad (21a)$$

$$D_{\perp} = \frac{4(6G + 1)\sigma^2}{9\pi^2} \eta \chi_0 V \sigma \approx 0.29 \eta \chi_0 V \sigma. \quad (21b)$$

Eq. (20) describes the effective motion of an ABP in the intermediate time scale, where the director remains fixed. Collisions cause its streaming velocity to decrease. But also, since collisions are stochastic, they generate diffusive motion with different diffusion coefficients in the longitudinal and transverse directions. A representation of this effective dynamics is shown in Fig. 1c.

Now, if we add back the rotational diffusion that takes place on a slower time scale, we obtain an effective Fokker-Planck equation for an ABP moving in a dense medium

$$\frac{\partial f}{\partial t} + V_{\text{eff}} \hat{\mathbf{n}} \cdot \nabla f = D_{\parallel} (\hat{\mathbf{n}} \cdot \nabla)^2 f + D_{\perp} (\hat{\mathbf{t}} \cdot \nabla)^2 f + D_r \nabla_{\hat{\mathbf{n}}}^2 f, \quad (22)$$

where collisions are taken into account in the effective coefficients V_{eff} , D_{\parallel} , and D_{\perp} .

On short time scales the motion is purely ballistic with the computed effective velocity, resulting in a mean square displacement (MSD) that goes as $\langle \Delta r^2 \rangle \sim V_{\text{eff}}^2 t^2$. Analogous results, modifying the MSD at short times due to interactions, have also been obtained for the self-diffusion process in single-file configurations³⁷.

Finally, it is possible to extend this description to an ensemble of ABPs, where each particle follows the stochastic dynamics associated with Eq. (22), but where now the coefficients depend on the local density field, representing mean-field interactions with the other particles. In this formalism, each particle is described by the Langevin equations

$$\dot{\mathbf{r}}_i = V_{\text{eff}}(\eta_i) \hat{\mathbf{n}}_i + \sqrt{2D_{\parallel}(\eta_i)} \xi_{\parallel,i} \hat{\mathbf{n}}_i + \sqrt{2D_{\perp}(\eta_i)} \xi_{\perp,i} \hat{\mathbf{t}}_i, \quad (23a)$$

$$\dot{\phi}_i = \sqrt{2D_r} \xi_{r,i}, \quad (23b)$$

where $\xi_{\parallel,i}$, $\xi_{\perp,i}$ and $\xi_{r,i}$ uncorrelated white noises, and η_i the coarse grained area fraction evaluated at \mathbf{r}_i . The mean-field interaction makes Eqs. (23)a-b significantly simpler than the original equations for ABPs interacting with hard-core repulsive pairwise potentials (1), both for theoretical and numerical analysis.

Both effective diffusion coefficients (21) are proportional to χ_0 , which is expected to diverge at close packing,

since collisions become infinitely frequent there. Therefore, both D_{\parallel} and D_{\perp} are predicted to diverge as well. This result is evidently wrong because at close packing no motion takes place. The origin of this discrepancy is the fact that the kinetic equation assumes from the very beginning the existence of binary collisions, which is not the case at high densities where many-body effects are present. Furthermore, Eq. (19) shows that the theory cannot be valid beyond $\eta\chi_0 = 1$. Indeed, beyond this density, the effective backward displacements due to collisions are larger than the free motion, resulting in a negative effective velocity. Using the elastic hard disk expression for the correlation function, this condition gives $\eta_{\max} \approx 0.42$.

V. LONG-TIME DIFFUSIVITY

For times greater than D_r , the tracer has completely forgotten its original direction and moves in an effective random walk. For isolated particles, this long-time diffusivity can first be estimated by dimensional analysis by noting that the particle performs a correlated motion with lengths $\ell = V/D_r$ for times lasting $\tau = D_r^{-1}$. This results in a diffusion coefficient that scales as $\ell^2/\tau = V^2/D_r$. Precise analytical calculations in Ref. 8 for isolated ABPs give the bare diffusivity $D_0 = V^2/(2D_r)$. In the presence of other particles, the velocity is effectively reduced as shown in the previous section, but collisional diffusive motion also appears. To obtain the long-time diffusion coefficient from the Lorentz equation (9), we again consider the van Hove process: the tracer is initially placed at the origin, but now with an isotropic distribution

$$f(\mathbf{r}, \hat{\mathbf{n}}, t = 0) = \delta(\mathbf{r})/(2\pi), \quad (24)$$

which is associated with an initial density $\rho(\mathbf{r}, t = 0) = \delta(\mathbf{r})$. Figure 1d represents this process schematically. In this regime, as the director evolves in time, it is not possible to obtain a closed expression for the van Hove function as in the previous section. Nevertheless, as we will show below, it is possible to compute the diffusion coefficient analytically with no approximation. To do this, we take advantage of the fact that the Laplace transform of the MSD can be computed in 2D as shown in Refs. 7 and 34,

$$\langle \widetilde{\Delta r^2} \rangle(s) = \lim_{k \rightarrow 0} \left(-2 \frac{\partial^2 \tilde{\rho}}{\partial k^2} \right). \quad (25)$$

At long times, the MSD should grow linearly with time $\langle \Delta r^2 \rangle(t) \sim 4Dt$, reflecting a diffusion process with diffusion coefficient D . Recalling that the Laplace transform of t is $1/s^2$, the diffusion coefficient can, therefore, be obtained as the s^{-2} coefficient of the Laurent series of the MSD in Laplace space

$$\langle \widetilde{\Delta r^2} \rangle(s) = \frac{4D}{s^2} + \sum_{n \geq -1} a_n s^n. \quad (26)$$

The objective then is to solve the kinetic equation in Fourier-Laplace space. From this, the procedure is to compute the van Hove function, then to obtain the MSD in Laplace space, and finally to derive the diffusion coefficient. Using the initial condition, the kinetic equation (9) for $\tilde{f}(\mathbf{k}, \hat{\mathbf{n}}_1, s)$, reads

$$s\tilde{f} - \frac{1}{2\pi} + iV\mathbf{k} \cdot \hat{\mathbf{n}}_1 \tilde{f} - D_r \frac{\partial^2 \tilde{f}}{\partial \phi_1^2} = \Phi \int [e^{-i\mathbf{k} \cdot \Delta_1} - 1] \tilde{f} dX. \quad (27)$$

To solve it, we use an expansion in Fourier angular modes

$$\tilde{f}(\mathbf{k}, \hat{\mathbf{n}}_1, s) = \frac{1}{2\pi} \sum_m g_m(\mathbf{k}, s) e^{im\phi_1}, \quad (28)$$

where the factor $1/2\pi$ is written for convenience, so that the van Hove function is $\tilde{\rho}(\mathbf{k}, s) = g_0(\mathbf{k}, s)$. Projecting the kinetic equation into the p mode and using $\mathbf{k} = k\hat{\mathbf{x}}$, we get

$$sg_p + \frac{ikV}{2}(g_{p+1} + g_{p-1}) + D_r p^2 g_p + \Phi \sum_m L_{pm} g_m = \delta_{p,0}, \quad (29)$$

which can be written as $\sum_m A_{pm} g_m = \delta_{p,0}$, defining the matrix \mathbb{A} . This gives $\tilde{\rho}(\mathbf{k}, s) = g_0 = [\mathbb{A}^{-1}]_{00}$. Here,

$$L_{pm} = \frac{1}{2\pi} \int e^{i(m-p)\phi_1} [1 - e^{-i\mathbf{k} \cdot \Delta_1}] \times |(\hat{\mathbf{n}}_2 - \hat{\mathbf{n}}_1) \cdot \hat{\boldsymbol{\sigma}}| \Theta[-(\hat{\mathbf{n}}_2 - \hat{\mathbf{n}}_1) \cdot \hat{\boldsymbol{\sigma}}] d\phi_1 d\phi_2 d\theta, \quad (30)$$

which depend only on $m - p$. First, without explicitly computing the matrix elements L_{pm} , it is possible using symbolic algebra softwares to obtain $\tilde{\rho}(\mathbf{k}, s)$ for increasing number of angular Fourier modes P , with expressions that depend on L_{pm} . Since we aim to compute the MSD via Eq. (25), we make a Taylor expansion in k of L_{pm} , by simply expanding the square bracket in the integral, which gives $L_{pm}(k) = L_{pm}^{(1)}k + L_{pm}^{(2)}k^2 + L_{pm}^{(3)}k^3 + \dots$, where it is directly verified by inspection that the constant terms vanish. This procedure gives for each P the MSD in Laplace space together with its Laurent series in s . The leading term goes as $L_{00}^{(1)}/s^3$, which would imply a superdiffusive t^2 behavior. Using the parametrization given in the Appendix, it is direct to compute the integrals and obtain that $L_{00}^{(1)}$ vanishes identically. In fact, this term is proportional to the collisional average of Δ_1 , which vanishes by isotropy. This results in the leading order in the MSD going, as expected, as $1/s^2$, which allows us to obtain the diffusion coefficient using Eq. (26)

$$D = \frac{V^2}{2D_r} + \Phi \left[L_{00}^{(2)} - \frac{iV}{2D_r} \left(L_{-1,0}^{(1)} + L_{0,-1}^{(1)} + L_{1,0}^{(1)} + L_{0,1}^{(1)} \right) - \sum_{m=1}^{\infty} \frac{L_{-m,0}^{(1)} L_{0,-m}^{(1)} + L_{m,0}^{(1)} L_{0,m}^{(1)}}{m^2 D_r} \right], \quad (31)$$

where we recognize the first term as the bare diffusivity D_0 for collisionless ABPs, while the second term results from the effect of collisions as it is manifest by the presence of the prefactor Φ , which is proportional to the cross section and the pair correlation function. Thus, to evaluate D , one needs to compute only a few matrix elements of order k^1 , and only L_{00} of order k^2 . Using the parametrization described in the Appendix, it is obtained that $L_{p,p\pm 1}^{(1)} = -i\pi^2\sigma/4$ and zero for the rest, which means that the sum in Eq. (31) stops at $m = 1$. Also, $L_{00}^{(2)} = 2G\sigma^2$. Collecting all terms gives

$$D = \frac{[V(1 - \rho_0\chi_0\pi^2\sigma/4)]^2}{2D_r} + G\rho_0\chi_0V\sigma^3/\pi. \quad (32)$$

The first term turns out to be simply the active diffusivity but now with the effective velocity V_{eff} given in Eq. (19). In dimensionless form $D = D_0(1 - \chi_0\eta)^2 + D_0\frac{8G\chi_0\eta}{\pi^2\text{Pe}}$. Since the kinetic theory we started with is valid only for high Péclet number, it is not consistent to consider the second term, and therefore the prediction of the theory reduces to

$$D = \frac{V_{\text{eff}}^2}{2D_r} = D_0(1 - \chi_0\eta)^2. \quad (33)$$

Notably, this dependence on the effective velocity has already been observed in numerical simulations of ABPs²³. As in the case of the dynamics at intermediate time scales, here the effective diffusion coefficient also depends on χ_0 . Also the theory fails at $\chi_0\eta = 1$, where D vanishes, but most likely the theory becomes quantitatively inaccurate for smaller densities.

Using the pair correlation function of elastic disks, it is possible to compute explicitly the long-term diffusivity for various values of the area fraction: $D(\eta = 0.1) \approx 0.78D_0$, $D(\eta = 0.2) \approx 0.51D_0$, and $D(\eta = 0.3) \approx 0.22D_0$, and $D(\eta = 0.4) \approx 0.007D_0$. These values can be compared with the numerical simulations in Ref. 23: $D(\eta = 0.1) \approx 0.82D_0$, $D(\eta = 0.2) \approx 0.64D_0$, and $D(\eta = 0.3) \approx 0.46D_0$, and $D(\eta = 0.4) \approx 0.28D_0$. This discrepancy, with computed values smaller than the measured ones suggest that the use of the equilibrium expression for the pair correlation function is a too crude approximation and it overestimates its real value.

VI. CONCLUSIONS

A recently proposed kinetic theory for interacting ABPs is used to study their self-diffusive dynamics. In the kinetic equation, the persistent excluded volume interactions between particles are described as effective particle displacements. To calculate the displacements, the kinetic theory assumes that the Péclet number is large, which implies that the directors of the particles do not change during collisions.

Starting from this kinetic equation, we consider the dynamics of a tagged particle, identical to the ABP bath,

which is in an equilibrium distribution. On intermediate time scales, where the director of the tagged particle remains fixed, the effective displacements produce an anisotropic diffusion, which is added to the streaming motion with an reduced effective velocity. This is summarized by the Fokker–Planck equation (22). Extending this description to an ensemble of interacting particles, this effective dynamics can be mapped to a set of Langevin equations where the particles now interact in a mean-field manner through the local density [Eqs. (23)a-b].

On larger time scales, where the director has had time to change, the dynamics is purely diffusive, with a diffusion coefficient given by Eq. (33) that accounts for all interaction effects. Notably, the long term diffusivity can be written as that of free particles, but now with the effective velocity.

The effective velocity becomes negative at large densities, which is clearly unphysical and affects the prediction on both intermediate and large timescales. Since the effective velocity was obtained without approximation from the kinetic theory, this implies that it is the kinetic theory that is limited to moderate densities. The vanishing of the effective velocity marks a strong maximum density for the theory to be valid, which using the pair correlation function of elastic hard disks gives $\eta \approx 0.42$. On the other hand, in Ref. 22 it was shown that the kinetic theory correctly predicts that the spinodal density for MIPS is $\eta \approx 0.25$ in two dimensions. These results imply that the present description is limited to moderate densities, quantitatively valid up to $\eta \approx 0.25$, to gradually deteriorate for increasing densities and to break down completely at $\eta \approx 0.42$. For area fractions higher than 0.25, the system will spontaneously separate into dilute and dense phases due to MIPS, and it is expected that the present calculations of self-diffusive motion remain valid as long as the density of the dense phase is not too high. Also, the numerical comparison of the long-term diffusivity with numerical simulations indicate that the equilibrium expression for the pair correlation function overestimates its value for ABPs. Further research is therefore needed to include, at least phenomenologically, many-body effects and the suppression of motion at high densities. This includes the study of the pair correlation function at contact for precollisional states and its possible angular dependence. If this is the case, and χ depends on the angles, the collisional integrals can be carried out according to the methods described above, modifying only the numerical values of the coefficients, which will depend on the explicit dependencies of χ .

In Ref. 38 it is shown that, similarly to equilibrium systems, for ABPs the long-time self-diffusivity D can be expressed in terms of the static structure factor and the isothermal compressibility. An interesting avenue of research is to investigate whether these relations remain valid within the framework of kinetic theory. Both density fluctuations and a protocol for calculating stresses in kinetic theory should be worked out, which are left for future work.

Finally, the results presented in this article are based on a kinetic theory that is limited to high Péclet numbers, and are therefore quantitatively correct only in this regime. The extension of the theory to finite Péclet needs to describe collisions stochastically, since the moment when the collision ends is a random variable. Ongoing research in this direction is on course and will be published elsewhere.

ACKNOWLEDGMENTS

This research was supported by the Fondecyt Grant No. 1220536 and Millennium Science Initiative Program NCN19_170 of ANID, Chile. R.S. thanks Ricardo Brito for inspiring discussions.

- ¹C. Bechinger, R. Di Leonardo, H. Löwen, C. Reichhardt, G. Volpe, and G. Volpe, “Active particles in complex and crowded environments,” *Reviews of modern physics* **88**, 045006 (2016).
- ²H. C. Berg, *Random walks in biology* (Princeton University Press, 1993).
- ³H. C. Berg, *E. coli in Motion* (Springer, 2004).
- ⁴B. Stramer and R. Mayor, “Mechanisms and in vivo functions of contact inhibition of locomotion,” *Nature reviews Molecular cell biology* **18**, 43–55 (2017).
- ⁵W. F. Paxton, K. C. Kistler, C. C. Olmeda, A. Sen, S. K. St. Angelo, Y. Cao, T. E. Mallouk, P. E. Lammert, and V. H. Crespi, “Catalytic nanomotors: autonomous movement of striped nanorods,” *Journal of the American Chemical Society* **126**, 13424–13431 (2004).
- ⁶A. Bricard, J.-B. Caussin, N. Desreumaux, O. Dauchot, and D. Bartolo, “Emergence of macroscopic directed motion in populations of motile colloids,” *Nature* **503**, 95–98 (2013).
- ⁷A. Villa-Torrealba, C. Chávez-Raby, P. de Castro, and R. Soto, “Run-and-tumble bacteria slowly approaching the diffusive regime,” *Physical Review E* **101**, 062607 (2020).
- ⁸J. R. Howse, R. A. Jones, A. J. Ryan, T. Gough, R. Vafabakhsh, and R. Golestanian, “Self-motile colloidal particles: from directed propulsion to random walk,” *Physical review letters* **99**, 048102 (2007).
- ⁹B. Lindner and E. Nicola, “Diffusion in different models of active brownian motion,” *The European Physical Journal Special Topics* **157**, 43–52 (2008).
- ¹⁰P. Romanczuk, M. Bär, W. Ebeling, B. Lindner, and L. Schimansky-Geier, “Active brownian particles: From individual to collective stochastic dynamics,” *The European Physical Journal Special Topics* **202**, 1–162 (2012).
- ¹¹S. Kumar, J. P. Singh, D. Giri, and S. Mishra, “Effect of polydispersity on the dynamics of active brownian particles,” *Physical Review E* **104**, 024601 (2021).
- ¹²G. Szamel and E. Fleener, “Extremely persistent dense active fluids,” *Soft Matter* **20**, 5237–5244 (2024).
- ¹³M. E. Cates and J. Tailleur, “When are active brownian particles and run-and-tumble particles equivalent? consequences for motility-induced phase separation,” *Europhysics Letters* **101**, 20010 (2013).
- ¹⁴A. P. Solon, M. E. Cates, and J. Tailleur, “Active brownian particles and run-and-tumble particles: A comparative study,” *The European Physical Journal Special Topics* **224**, 1231–1262 (2015).
- ¹⁵Y. Fily and M. C. Marchetti, “Athermal phase separation of self-propelled particles with no alignment,” *Physical review letters* **108**, 235702 (2012).
- ¹⁶G. S. Redner, M. F. Hagan, and A. Baskaran, “Structure and dynamics of a phase-separating active colloidal fluid,” *Physical review letters* **110**, 055701 (2013).
- ¹⁷D. Levis and L. Berthier, “Clustering and heterogeneous dynamics in a kinetic monte carlo model of self-propelled hard disks,” *Physical Review E* **89**, 062301 (2014).
- ¹⁸Y. Fily, S. Henkes, and M. C. Marchetti, “Freezing and phase separation of self-propelled disks,” *Soft matter* **10**, 2132–2140 (2014).
- ¹⁹P. Digregorio, D. Levis, A. Suma, L. F. Cugliandolo, G. Gonnella, and I. Pagonabarraga, “Full phase diagram of active brownian disks: From melting to motility-induced phase separation,” *Physical review letters* **121**, 098003 (2018).
- ²⁰J. Tailleur and M. Cates, “Statistical mechanics of interacting run-and-tumble bacteria,” *Physical review letters* **100**, 218103 (2008).
- ²¹M. E. Cates and J. Tailleur, “Motility-induced phase separation,” *Annu. Rev. Condens. Matter Phys.* **6**, 219–244 (2015).
- ²²R. Soto, M. Pinto, and R. Brito, “Kinetic theory of motility induced phase separation for active brownian particles,” *Phys. Rev. Lett.* **132**, 208301 (2024).
- ²³J. Wang, “Anomalous diffusion of active brownian particles in crystalline phases,” in *IOP Conference Series: Earth and Environmental Science*, Vol. 237 (IOP Publishing, 2019) p. 052005.
- ²⁴J. Reichert and T. Voigtmann, “Tracer dynamics in crowded active-particle suspensions,” *Soft Matter* **17**, 10492–10504 (2021).
- ²⁵S. Chapman and T. G. Cowling, *The mathematical theory of non-uniform gases: an account of the kinetic theory of viscosity, thermal conduction and diffusion in gases* (Cambridge university press, 1990).
- ²⁶R. Soto, *Kinetic theory and transport phenomena* (Oxford University Press, 2016).
- ²⁷H. Van Beijeren and M. H. Ernst, “The modified enskog equation,” *Physica* **68**, 437–456 (1973).
- ²⁸N. Brilliantov and T. Pöschel, *Kinetic theory of granular gases* (Oxford University Press, 2004).
- ²⁹V. Garzó, *Granular gaseous flows* (Springer, 2019).
- ³⁰R. Soto and M. Mareschal, “Statistical mechanics of fluidized granular media: Short-range velocity correlations,” *Physical Review E* **63**, 041303 (2001).
- ³¹N. de Macedo Binossek, H. Löwen, T. Voigtmann, and F. Smallenburg, “Static structure of active brownian hard disks,” *Journal of Physics: Condensed Matter* **30**, 074001 (2018).
- ³²J. Jeggle, J. Stenhammar, and R. Wittkowski, “Pair-distribution function of active brownian spheres in two spatial dimensions: simulation results and analytic representation,” *The Journal of Chemical Physics* **152** (2020).
- ³³D. Henderson, “A simple equation of state for hard discs,” *Molecular Physics* **30**, 971–972 (1975).
- ³⁴J. P. Boon and S. Yip, *Molecular hydrodynamics* (Courier Corporation, 1991).
- ³⁵J. Bialké, H. Löwen, and T. Speck, “Microscopic theory for the phase separation of self-propelled repulsive disks,” *Europhysics Letters* **103**, 30008 (2013).
- ³⁶T. A. de Pirey, G. Lozano, and F. Van Wijland, “Active hard spheres in infinitely many dimensions,” *Physical review letters* **123**, 260602 (2019).
- ³⁷A. Akintunde, P. Bayati, H. Row, and S. A. Mallory, “Single-file diffusion of active brownian particles,” *arXiv preprint arXiv:2411.08988* (2024).
- ³⁸A. R. Dulaney, S. A. Mallory, and J. F. Brady, “The ‘isothermal’ compressibility of active matter,” *The Journal of Chemical Physics* **154** (2021).

Appendix A: Effective displacements and collision parametrization in two spatial dimensions

Here, for completeness, we copy from Ref. 22 the expressions for the effective displacements and the form the collisional integrals are computed. In two dimensions, collisions are parametrized by the angles ϕ_1 and ϕ_2 of the two directors, and θ the angle formed by the unit vector $\hat{\sigma}$ and $\hat{\mathbf{n}}_2 - \hat{\mathbf{n}}_1$ at the beginning of the collision, such that $\cos \theta < 0$, as shown in Fig. 2.

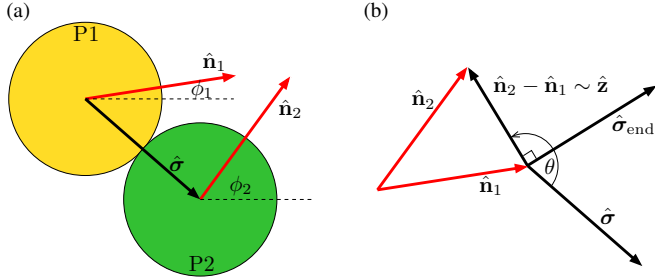


FIG. 2. Geometry of the collision of particles P1 and P2. (a) The particle directors $\hat{\mathbf{n}}_1$ and $\hat{\mathbf{n}}_2$ are parametrized by the angles $\phi_{1,2}$, respectively, measured with respect to a fixed horizontal axis. The unit vector $\hat{\sigma}$ points from particle 1 to particle 2 at the beginning of the collision. (b) $\hat{\sigma}$ is parametrized with the angle θ , which it forms with $\hat{\mathbf{z}} = (\hat{\mathbf{n}}_2 - \hat{\mathbf{n}}_1)/|\hat{\mathbf{n}}_2 - \hat{\mathbf{n}}_1|$. At the end of the collision, the unit vector from particle 1 to particle 2 is $\hat{\sigma}_{\text{end}}$.

Integrating the equations of motion it results that the duration of the collision is²²

$$\Delta t^{\text{col}} = \frac{\sigma}{V|\hat{\mathbf{n}}_2 - \hat{\mathbf{n}}_1|} \log |\tan(\theta/2)|, \quad (\text{A1})$$

and two situations can take place for the angle θ_{end} at the end of the collision. If $\pi/2 \leq \theta < \pi$, $\theta_{\text{end}} = \pi/2$, but if $\pi < \theta \leq 3\pi/2$, $\theta_{\text{end}} = 3\pi/2$. With this, writing the

directors as $\hat{\mathbf{n}}_i = (\cos \phi_i, \sin \phi_i)$, the unit vectors can be written as

$$\hat{\sigma} = R(-\theta)\hat{\mathbf{z}}, \quad (\text{A2})$$

and

$$\hat{\sigma}_{\text{end}} = \begin{cases} R(-\pi/2)\hat{\mathbf{z}}, & \pi/2 \leq \theta < \pi \\ R(\pi/2)\hat{\mathbf{z}}, & \pi < \theta \leq 3\pi/2, \end{cases} \quad (\text{A3})$$

where $\hat{\mathbf{z}} = \left(\frac{\cos \phi_2 - \cos \phi_1}{\sqrt{2 - 2 \cos(\phi_2 - \phi_1)}}, \frac{\sin \phi_2 - \sin \phi_1}{\sqrt{2 - 2 \cos(\phi_2 - \phi_1)}} \right)$ is the unit vector parallel to $(\hat{\mathbf{n}}_2 - \hat{\mathbf{n}}_1)$ and $R(\alpha) = \begin{pmatrix} \cos \alpha & -\sin \alpha \\ \sin \alpha & \cos \alpha \end{pmatrix}$ is the rotation matrix. Finally, the effective displacements are

$$\Delta_1 = -\sigma \frac{\hat{\sigma}_{\text{end}} - \hat{\sigma}_0}{2} - V \Delta t^{\text{col}} \frac{\hat{\mathbf{n}}_1 - \hat{\mathbf{n}}_2}{2}, \quad (\text{A4})$$

$$\Delta_2 = -\Delta_1. \quad (\text{A5})$$

With this parametrization, the different expressions needed to compute the integrals can be easily expressed in terms of ϕ_1 , ϕ_2 , and θ . For example,

$$|\hat{\mathbf{n}}_2 - \hat{\mathbf{n}}_1| = \sqrt{2 - 2 \cos(\phi_1 - \phi_2)}, \quad (\text{A6})$$

$$(\hat{\mathbf{n}}_2 - \hat{\mathbf{n}}_1) \cdot \hat{\sigma} = \sqrt{2 - 2 \cos(\phi_1 - \phi_2)} \cos \theta, \quad (\text{A7})$$

$$|(\hat{\mathbf{n}}_2 - \hat{\mathbf{n}}_1) \cdot \hat{\sigma}| \Delta_1 = \frac{\sigma |\cos \theta|}{2} \left\{ \begin{aligned} & [\cos(\phi_2 - \theta) - \cos(\phi_1 - \theta) + (\cos \phi_2 - \cos \phi_1) \log |\tan(\theta/2)| \\ & \pm (\sin \phi_1 - \sin \phi_2)] \hat{\mathbf{x}} + [\sin(\phi_2 - \theta) - \sin(\phi_1 - \theta) \\ & + (\sin \phi_2 - \sin \phi_1) \log |\tan(\theta/2)| \pm (\cos \phi_2 - \cos \phi_1)] \hat{\mathbf{y}} \end{aligned} \right\}, \quad (\text{A8})$$

where the positive sign is for $\pi/2 \leq \theta < \pi$ and the negative one for $\pi < \theta \leq 3\pi/2$.